The Indonesian Journal of Computer Science
www.ijcs.net
Volume 14, Issue 2, April 2025
https://doi.org/10.33022/ijcs.v14i2.4757

Development of Sensor System based on Air Pressure for Robot Leg Contact Detection

Wahyu Agung Dwi Prasetyo[1], Adytia Darmawan[2], Raden Sanggar Dewanto[3], Khairurizal Alfathdyanto[4]
wahyuhagung@me.student.pens.ac.id[1], adytia@pens.ac.id[2], sanggar@pens.ac.id[3], khairurizal@pens.ac.id[4]
[1,2,3,4] Electronic Engineering Polytechnic Institute of Surabaya

Article Information

Received : 24 Feb 2025
Revised : 25 Apr 2025
Accepted : 30 Apr 2025

Keywords

Robot leg, Air pressure sensor, Robot footprint, Leg contact detection,

Abstract

Legged robot is preferred choice for travesing uneven terrain. Robot leg can be positioned dynamically to achieve better locmotion. Detection of the leg contact point became more of essential part for the unpredictable course. The common method by deploying resistive force sensor provides a binary condition of whether the leg has touches surface. This paper explores the possibility of implementing air pressure sensor on a sensor system to provide more information at robot leg contact point. Air pressure sensor can provide a more wide and continuous range of value that fluctuates along the contact rate of the leg. Verification of the study uses single leg part of dog-type quardruped. The sensor testing gave the output value with average error of 1,3%. The pressure sensor provides readings at around ± 40ms with maximum readable pressure of 1,5 kPa.

A. Introduction

Legged robots is a continously developed technology with more focused on dynamics control. Thanks to understanding of locomotion an movement capabilities, motion algorithms could be improve to adapt to more natural dynamic modeled after animal gait patterns. The more complexity of dynamic movement such walking or running, the more require for computation which demand a high performance process [1]. The development of search and rescue robots in authors campus follows the Indonesian robot contest in which the robot is required to pass several obstacle. The quadruped robot has been developed including hazardous environment such as inclined obstacle, stairwells, flatbed obstacle and uneven obstacle.

Legged robot especially quadruped excels in traversing various terrain as such in the competition the robot had to pass obstacle such as stairs, marbles and cracked terrain to complete the mission. There are several reasons why robot can not complete the mission. Some participant use various gait but This method is not enough to pass stair obstacle. While on the stair obstacle robot could slip because the pressure from each foot was not well distributed. Therefore, the author assumed that the pose of robot would be pivotal in tackling the problem.

Quadruped locomotion would be affected mainly by the gait that is currently implemented in action [2]. Gait is a common approach to achieve legged robot locomotion [3]. Gait comprises of sequence of robot pose that would be executed each timeframe. This is a popular option to simplify legged robot locomotion. However, this pre-determined set of moves has limitations for applicable terrain. The issue urges author to implement an adaptive solution for the robot locomotion. However without proper sensing mechanism, the movement would solely rely on this established gaits.

State-estimation is an alternative aside from implementing leg contact sensor. However, there is a noticeable drift in state estimation between soft and rough terrain [4]. Therefore, contact sensors would be preferable for more accurate application. One of popular approach uses force sensitive resistor [5]. FSR is a component that gives simple-reading upon contact. The reading of FSR usually determines whether the leg is already on contact [6], in another word binary. Some other method is also explored such as low-cost binary-contact sensor based on rubber displacement [7], contact sensor with LED emitter and receiver [8], vision-based multi-functional sensor foot [9] in recent researches. We would proposed a novel foot design with elastic tip that can be sensed using pressure-based sensors upon contact.

In this work, we designing a unique leg to developed, based on anatomy real dog. This design allows for movement that closely the leg of real dogs. For the starter, we use elastic material from silicone rubber for the end of robot leg. This provides more grip to uneven terrain especially in stairs. The vessel also have an air pocket that compresses as it touches the ground. Air pressure sensor detects changes from the compressed vessel and gives its reading for the microcontroller. Authors also implements FSR in conjunction to compare the results with the more general approach. To validate our sensor development, we deployed on a singular leg of the robot and plant the sensor system into it.

The purpose of this was to add and develop the sensor to analyze the pattern of the robot's footprint, manufacture the design, and apply a quadruped robotic leg mechanism. This paper is devide into five section. Section B explains the methods underlying the sensor system and the inverse kinematics of the robot leg. In section C, we describe design of the robot leg for implementation. In section D, we analyze the result when implemented on the leg robot. In section E, we evaluate our work and discuss future work.

B. Research Method

B.1 Pressure Sensor

The pressure sensor was a device to measure fluid or gas pressure in a system. This sensor functioned to convert mechanical pressure into electrical signal that could be measured and produce an appropriate output signal.

The model for measuring pressure used an FSR type FSR402, which was capable of measuring pressure up to 2 KG. The sensor sensor readings were designed using the concept of a voltage divider circuit. This voltage divider circuit was connected to the Analog to Digital Converter (ADC) on the microcontroller, so the voltage divider circuit consisted of one resistor with a variable value to be tested. The FSR as a varying resistor , and a 5V power supply according to the working voltage of the microcontroller. The circuit of the FSR is shown in Figure 1.

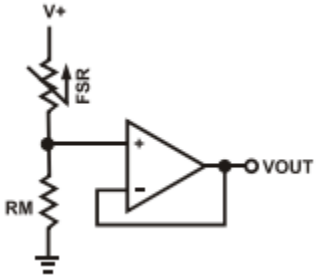

Figure 1. FSR Circuit

The FSR device was tied to a measuring resister in a voltage divider configuration. The output was described by the equation:

$$Voltage\ Divider = \frac{(Resistor\ Value)}{(FSR\ Value + Resistor\ Value)} \times Voltage\ input \quad (1)$$

In the shown configuration the output voltage increased the desired force sensitivity range and to limit current. The current through the FSR should be limited to less than 1 mA/cm of force applied. The op-amp used for the design was the LM324. The low bias current of this op-amp reduces errors due to source impedance voltage divider.

B.2 Air Pressure Sensor

The air pressure sensor used is MPX10DP with a Pressure reading of 0 to 10 Kpa, at full scale this sensor readout is up to 35mA.

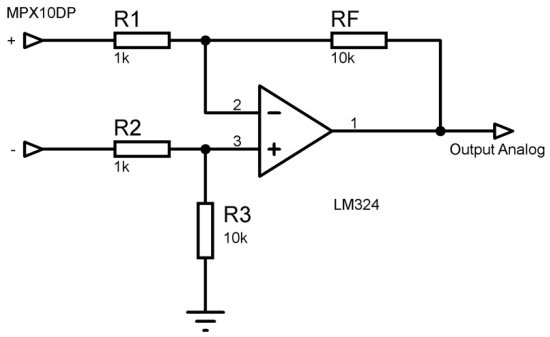

Figure2. Schematic MPX10DP with op-amp

The circuit design in the use of op-amps is required to strengthen the stand of the MPX10DP sensor output by utilizing the amplifier configuration. Requirement for output at op-amp gain:

$$V_{out} = \left(\frac{R_F}{R_1}\right)(V_{MPX+} - V_{MPX-}) \quad (2)$$

Identify resistance values:
R_F = 10K
R_1 = 1K

Calculating the gain value:

$$Gain = \frac{R_F}{R_1} \quad (3)$$

Amount of resistance given:

Gain=10K/1K=10

The gain of the circuit is 10 times. Gain on the op-amp aimed to make the output value of the MPX10DP sensor readable by the microcontroller. The output value the came directly from the sensor was only a few millivolts, about 0,1 mV, so it could not be read by the microcontroller. The op-amp also served to stabilized the output data.

B.3 Invers kinematic

According to the formation of the Coordinate system, the O_b coordinate system was defined as the global coordinate, fixed to the ground. The body part in the O_b coordinate was located at the geometric center of the robot's body, where X_b was

forward direction of the robot and Z_b the inverse direction of gravitational acceleration. The coordinate systems $O_{k1}, O_{k2}, O_{k3}, O_{k4}$ (with K = 1,2,3,4 respectively) were located at the rotational joint of each of the four legs and at the tip of the leg. To simplify subsequent calculation, the orientation of the coordinate system was defined identically for parameter differing. Coordinate system orientation can be seen on Figure 3.

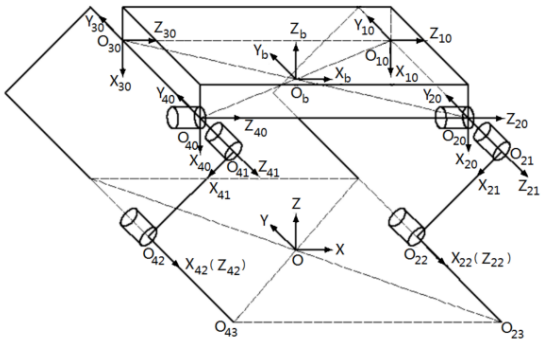

Figure3. Coordinate System Diagram

In this method, each link describe by four link parameters. When the coordinate system i was applied to each link parameter, the following definition were found:

a_i= Distance from Z_i to Z_{i+1} along X_i axis
α_i= Rotation angle around the X_i axis, from Z_i to Z_{i+1}
d_i = Distance along the Z_i axis, from X_{i-1} to X_i
θ_i = Rotation angle around the Z_i axis, from X_{i-1} to X_i

When solving equations using this method, these equations were usually decomposed into sub-problems. The coordinate system transformation from link i-1 to link i resulted in transformation matrix that connected the four parameters. Based on the definitions of each link parameter above, based on the definitions of each link parameter above.

$$ {}^{i-1}_{i}T = Trans_x\{a_{i-1}\}Rot_x\alpha_{i-1}Trans_z\{d_i\}Rot_x\{\theta_i\} \quad (4) $$

Used right leg for explain, so:

$$ {}^{0}_{4}T = \begin{bmatrix} c\theta_1 c(\theta_2+\theta_3) & -c\theta_1 s(\theta_2+\theta_3) & -s\theta_1 & a_2 c\theta_1 c\theta_2 - a_1 s\theta_1 + a_3 c\theta_1 c(\theta_2+\theta_3) \\ s\theta_1 c(\theta_2+\theta_3) & s\theta_1 s(\theta_2+\theta_3) & c\theta_1 & a_1 c\theta_1 - a_2 s\theta_1 s\theta_2 + a_3 c\theta_1 c(\theta_2+\theta_3) \\ -s(\theta_2+\theta_3) & -c(\theta_2+\theta_3) & 0 & -a_3 s(\theta_2+\theta_3) - a_2 s\theta_2 \\ 0 & 0 & 0 & 1 \end{bmatrix} \quad (5) $$

Matrix transformation from coordinate system $\{O_{20}\}$for

$$ {}^{b}_{20}T = \begin{bmatrix} 0 & 0 & 1 & b \\ 0 & 1 & 0 & -w \\ -1 & 0 & 0 & 0 \\ 0 & 0 & 0 & 1 \end{bmatrix} \quad (6) $$

Transformation from coordinate system leg footprint O_{24} from right leg footprint to O_b founded. This gives forward kinematic equation for front right leg. According to invers kinematic solution;

$$ {}^{0}_{4}T = {}^{0}_{1}T\,{}^{1}_{2}T\,{}^{2}_{3}T\,{}^{3}_{4}T \quad (7) $$

After simplification, one can get equation:

$$ (x_0 c\theta_1 + y_0 s\theta_1)c\theta_2 - z_0 s\theta_2 = a_1 + a_3 c\theta_3 \quad (8) $$

$$ -(x_0 c\theta_1 + y_0 s\theta_1)s\theta_2 - z_0 s\theta_2 = a_3 c\theta_3 \quad (9) $$

$$ y_0 c\theta_1 - x_0 s\theta_1 - a_1 = 0 \quad (10) $$

The solution are:

$$ \theta_1 = \sin^{-1}\left(-\frac{a_1}{\sqrt{x_0^2 + x_0^2}}\right) + \phi \quad (11) $$

$$ \theta_2 = \pm \sin^{-1}\left(\frac{a_1 s\theta_3}{\sqrt{(x_0 c\theta_1 + y_0 s\theta_1)^2 + z_0^2}} - \alpha\right) \quad (12) $$

$$ \theta_3 = \pm \cos^{-1}\left(\frac{(x_0 c\theta_1 + y_0 s\theta_1) + z_0^2 - a_2^2 - a_3^2}{2a_2 a_3}\right) \quad (13) $$

The Above equation, the solution to the system of inverse kinematic equation for the right front leg, where θ_2 is taken as positive and θ_3 as negative drawn.

C. Manufacture Processes

C.1 Robot Leg Design

Robot design has a total DoF of 12 Degress of Freedom (DoF). But for this case, the used one leg with 3 DoF and sensor that had been installed. As shown in Figure 4. Shows the front and side view of mechanical leg of quadruped robot. Mechanical design using Inventor software and the material using 3D printed component and 2mm alumunium.

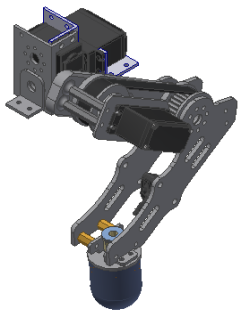

Figure4. Robot Leg Mechanical Design

C.2 Hardware of Quadruped robot

The hardware includes microcontroller, sensor in board design. The main controller runs robot performance ranging from accesing sensor and kinematic. the data read from pressure sensor is an ADC, since the result is analogue data, it needs to be converted to pressure unit. System diagram shown in Figure 5.

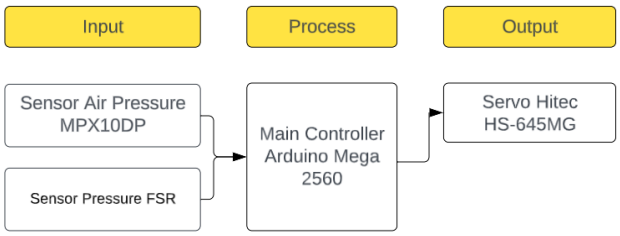

Figure5. Electrical System Block Diagram

Hardware design consisted of an Air Pressure MPX10DP and FSR402 as the sensor, an Arduino Mega 2560 as the controller, and Hitec HS-645MG Servo as an actuator. MPX10DP sensor was used for detect air pressure that in inside of the robot's footprint. FSR402 was used to read for the force pressure value on the toe. Process data using Arduino Mega 2560 which is read via analog pin and command are sent to servo using PWM pin. The sensor mechanism was made by combining the MPX10DP air pressure sensor with the FSR402 pressure.

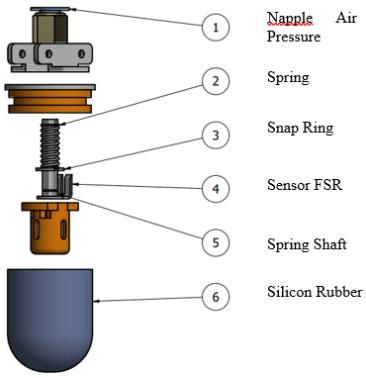

Figure6. Sensor System Components

The robot's footprint mechanism was made using silicone rubber in a halfcircular shape. This was done so that air pressure sensor could take pressure readings from all side wirhin a half-circle radius. Robot has footprint mechanical design shown in Figure 6. The material used for frame robot is aluminium and 3D Print filament PLA. This robot has four-legged with 3 DoF (Degree of Freedom) each. Making easy in movement.

C.3 Manufacturing Process

The quadruped robot had several components made from different materials. Fabrication and assembly can be seen in Figure 7. There were many methods and

types of machines used in the manufacturing process. the researchers used contouring, drilling, and pocketing. The leg joints were connected by aluminum, and the tips of the legs used the robot footprint mechanism covered by silicone rubber. This was done to prevent the robot's legs from slipping and to withstand air pressure on the robot's feet.

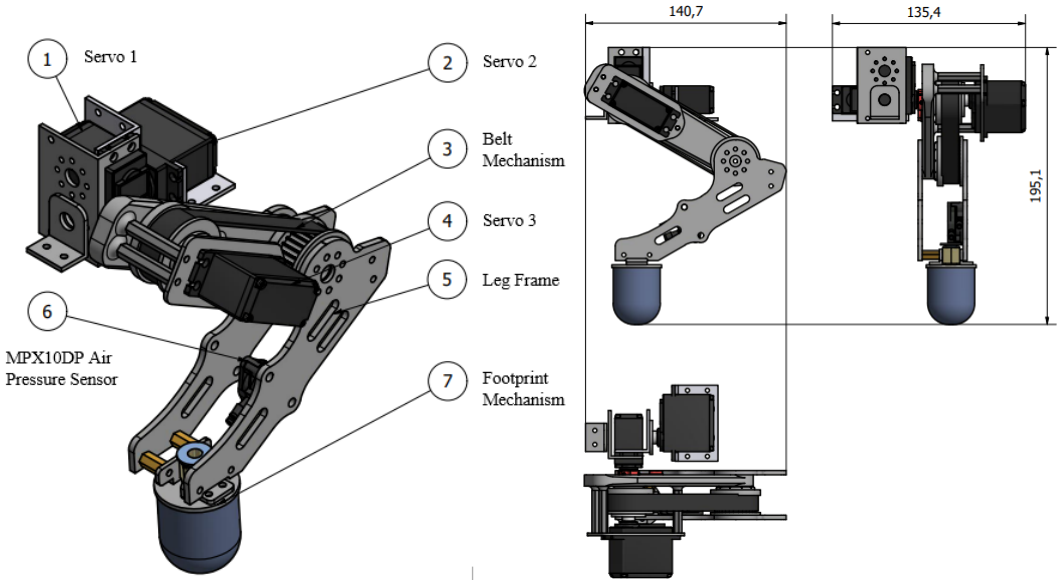

Figure7. 3D view of Robot Leg (a) and mechanical drawing (b)

Mechanical structural design was shown in Figure 7b. There are are 3 degrees of freedom (DoF) are implemented the joint of each leg. A mechanical structure is also designed that considered quadruped robot can walk forward, turn left and right. Figure 8 shows the overall quadruped leg robot implementation.

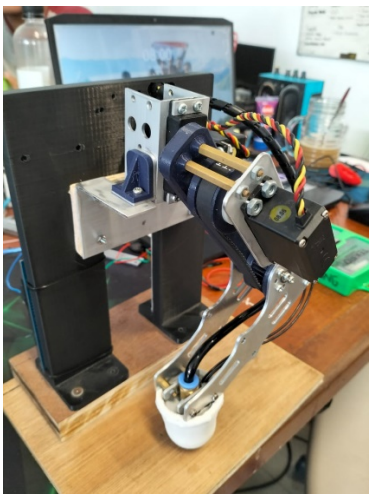

Figure8. Manufactured Robot Leg

D. Result and Discussion

D.1 Pressure Sensor Component Testing

Figure9. Testing MPX10DP Sensor

To ensure the MPx10DP sensor functioned properly on the robot and to access its response speed, testing was conducted by attaching the sensor to a syringe to determine its readings at each kPa. The sensor, capable of measuring air pressure up to 10 kPa, was already installed on the robot's leg. Minimum and maximum output values were recorded the leg module, as shown in figure 10.

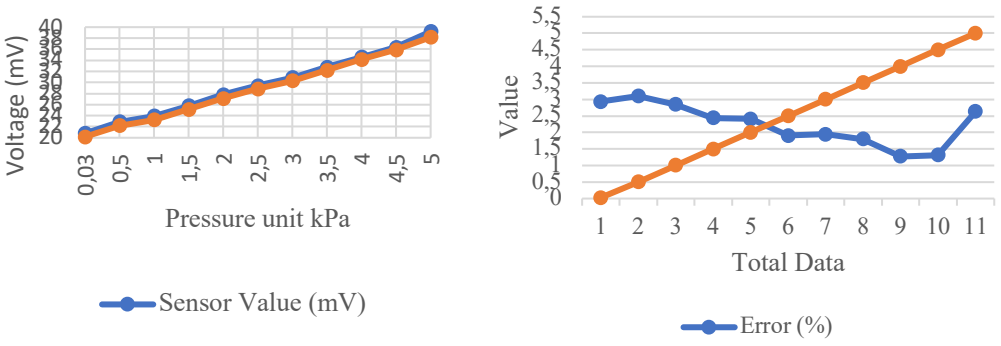

Figure10. Testing Result of MPX10DP

This was a comparison of the sensor value (which was read via the multimeter) with the sensor (Arduino serial monitor). This value was converted into Kpa units so that data for each kPa was 4 Milivolt. This testing was conducted only until the signal output limit was 50mV in which the average error was calculated at 1,3%. Also, the limit of readable pressure would be rated at 1,5 kPa for this component. This was done to maintain the accuracy of the sensor readings. Testing was conducted by applying pressure to the robot's foot made of silicone. The analysis of the test results will help in understanding how the MPX10DP pressure sensor respond to the pressure applied to the robot's foot. The generated under various conditions and to understand the pressure change patterns on each robot leg to stimulate actual robot conditions.

D.2 FSR Testing

Testing was on robot foot. The sensor installed in each foot. In this test, the input voltage value in the FSR circuit is 5 Volt.

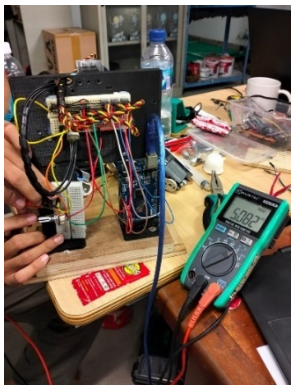

Figure11. FSR Sensor Testing

In this test, the input voltage value in the FSR was 5 Volt. Before testing the robot's legs FSR sensor's resistance measurement ranged from a minimum of 1K Ohm to a maximum of 1M Ohm. After installation on the robot leg, the FSR sensor had a minimum resistance value of 2,4K Ohm (when the leg was pressed). This change occurred because the value was damped by the built-in silicone rubber integrated with the sensors.

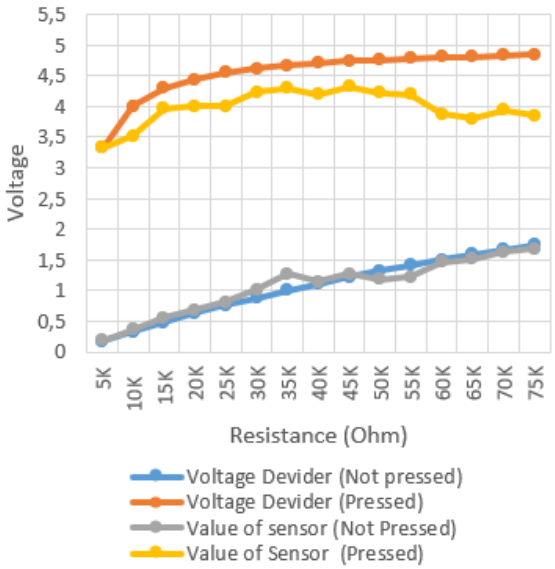

Figure12. FSR Testing Result

FRS testing in the data collection was based on equation [1]. The difference between equation and the FSR sensor readings could be seen in graph. The sensor testing showed that the output value range when pressed was influenced by the value of the resistor used. Within this range the robot could determine the condition of the leg when it was stepping or lifted. The results of the comparison

between the sensor measurements and the equation showed a percentage error, which can be seen in graph. The error range was from 0.8 to 1.25. The differences in the sensor readings were caused by the condition of the sensor mounted on the robot foot.

D.3 Trajectory Testing

The robot is said to be moving if it meets the values of the robot's trajectory and sensor data. In stepping, the robot is required to use the Z variable to lift the foot. After the foot moves forward.

Figure13. Trajectory Implementation on Robot Leg

Retrieval of air sensor output data is in the form of ADC values displayed on the monitor. The air pressure that appears is caused by pressing the silicone rubber on the robot's legs. The resulting data can be used to understand the pressure response and performance of the robot in various conditions, as well as read the pattern of changes in pressure on the robot's legs during pressure conditions. Different graphic patterns with pressing conditions produce actual robot conditions.

The sensor data value is used to determine the surface to be stepped on to form a semi-circular foot pattern. This difference in pattern indicates the pressure received on the robot's legs during movement. This data can be used to improve the robot's stability while in motion.

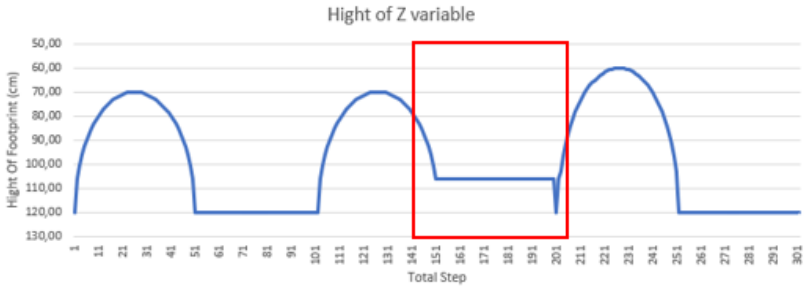

Figure14. FSR Sensor Testing

The serial plotter. In the condition where the foot is treading, it is shown in the red box. Changes in the foot pattern are triggered by the reading value from the

sensor. After that there is a change in Z height. In this graph, 1 step consists of 50 steps. The foot pattern creates a semicircular pattern with the lowest point at 70 mm and the highest point at 120 mm. In sensor testing, there is an interrupt to stop steps at a certain position. From this data and trajectory graph, it can be concluded that the control system on the quadruped robot legs with 3 DOF can maintain height when detecting pressure by sensors, the robot leg servo maintains its position before stepping higher to avoid obstacles. This shows that improvements in foot design and especially in the footpin mechanism have provided better movement.

E. Conclusion

An experimental approach for performance of a sensor pressure on quadruped was carried out in this research. Pressure sensor testing is used in this research. Here is summary of the findings. Pressure sensing test for MPX10DP able to provide signal to the controller and is successfully read within ± 40ms. The output value the op -amp has an average error of 1,3%. The limitation of the current design has a maximum readable pressure of 1,5 kPa. Change in the voltage value on the FSR are influenced by the value of the resistor in the voltage divider circuit.

F. Acknowledgment

The local research grant from EEPIS supported the production of this article. Hopefully, the advancement in this research helped in contribution towards EEPIS achievements.

G. References

[1] N. T. Thinh, N. T. V. Tuyen, and D. T. Son, "Gait of quadruped robot and interaction based on gesture recognition," J. Autom. Control Eng., vol. 4, no. 1, pp. 53–58, Feb. 2016.

[2] A. Majithia et al., "Design, motions, capabilities, and applications of quadruped robots: a comprehensive review," Front. Mech. Eng., vol. 10, 2024. doi: 10.3389/fmech.2024.1448681.

[3] W. Chou, T. Wang, and L. Hu, "Design of data glove and arm type haptic interface," in Proc. 11th Symp. Haptic Interfaces Virtual Environ. Teleoperator Syst., Los Angeles, CA, USA, 2003, pp. 422–427. doi: 10.1109/HAPTIC.2003.1191332.

[4] S. Fahmi, G. Fink, and C. Semini, "On state estimation for legged locomotion over soft terrain," IEEE Sensors Lett., vol. 5, no. 1, pp. 1–4, Jan. 2021, Art no. 6000104. doi: 10.1109/LSENS.2021.3049954.

[5] X. Guan and X. Zhao, "Design and signal processing of the legged robot foot tip pressure sensor," in Proc. 11th World Congr. Intell. Control Autom., Shenyang, China, 2014.

[6] Y. Takei, K. Morishita, R. Tazawa, and K. Saito, "Active gaits generation of quadruped robot using pulse-type hardware neuron models," Biomimetics, IntechOpen, Jun. 9, 2021. doi: 10.5772/intechopen.95760.

[7] H. Nam, Q. Xu, and D. Hong, "A reliable low-cost foot contact sensor for legged robots," in Proc. 17th Int. Conf. Ubiquitous Robots (UR), Kyoto, Japan, 2020, pp. 219–224. doi: 10.1109/UR49135.2020.9144878.
[8] F. Grimminger et al., "An open torque-controlled modular robot architecture for legged locomotion research," IEEE Robot. Autom. Lett., vol. 5, no. 2, pp. 3650–3657, Apr. 2020. doi: 10.1109/LRA.2020.2976639.
[9] G. Shi, C. Yao, X. Liu, Y. Zhao, Z. Zhu, and Z. Jia, "Foot vision: A vision-based multi-functional sensorized foot for quadruped robots," IEEE Robot. Autom. Lett., vol. 9, no. 7, pp. 6720–6727, Jul. 2024. doi: 10.1109/LRA.2024.3408084.
[10] Y. Shi, S. Li, M. Guo, Y. Yang, D. Xia, and X. Luo, "Structural design, simulation and experiment of quadruped robot," Appl. Sci., vol. 11, no. 22, p. 10705, 2021.
[11] A. Kusuma, "Desain dan implementasi sistem sensor tubing foot contact switch pada robot SAR," J. Teknol. Robot., vol. 8, no. 2, pp. 45–52, 2022.
[12] W. Sun et al., "Balance control of a quadruped robot based on foot fall adjustment," Appl. Sci., vol. 12, no. 5, p. 2521, Feb. 2022.
[13] M. Silva, P. Costa, and R. Ferreira, "Adaptive control strategies for a quadruped robot in rough terrain," Int. J. Adv. Robot. Syst., vol. 16, no. 1, pp. 1–13, 2019.
[14] J. Lee, S. Kim, and H. Oh, "Sensor fusion and control for robust locomotion in a quadruped robot," IEEE Trans. Robot., vol. 36, no. 5, pp. 1472–1485, 2020.
[15] M. Park, K. Kim, and S. Lee, "Autonomous quadruped robot with advanced terrain adaptation capabilities," J. Field Robot., vol. 38, no. 4, pp. 512–530, 2021.
[16] Y. Liu, R. Feng, and J. Sun, "FSR sensor-based tactile sensing system for quadruped robots: design and experimentation," IEEE Trans. Mechatronics, vol. 27, no. 3, pp. 1421–1431, 2022.
[17] K. Saputra, K. Takesue, K. Wada, A. J. Ijspeert, and N. Kubota, "Aquro: A cat-like adaptive quadruped robot with novel bio-inspired capabilities," Front. Robot. AI, vol. 8, p. 562524, 2021.Z.